DOI:10.1021/jf803948g

JOURNAL OF AGRICULTURAL AND FOOD CHEMISTRY
ARTICLE

Dose-Dependent Absorption and Metabolism of *trans*-Polydatin in rats

Siyuan Zhou,[†] Runtao Yang,[†] Zenghui Teng,[†] Bangle Zhang,[†] Yuzhen Hu,[†] Zhifu Yang,[†] Menglei Huan,[†] Xiang Zhang,[#] and Qibing Mei[§,*]

[†] Department of Pharmaceutics, [§]Department of Pharmacology, School of Pharmacy, and [#] Department of Neurosurgery, Xijing Hospital, Fourth Military Medical University, Xi'an 710032, China

There is considerable evidence that stilbenes provide health benefits. *trans*-Polydatin is one of the major stilbenoid compounds in red wine. The purpose of this study is to investigate the dose-dependent absorption and metabolism of *trans*-polydatin in rats. *trans*-Polydatin was administered to rats by gavage at three different doses (50, 100, and 300 mg·kg^{-1}). Blood samples were then collected at different time points. In situ perfusion of rat small intestine and liver was used to investigate the first-pass metabolism of *trans*-polydatin. *trans*-Polydatin and its metabolites were detected by LC-MS/MS. *trans*-Polydatin and its metabolites resveratrol, glucuronidated resveratrol, and glucuronidated *trans*-polydatin were detected in plasma within 10 min following oral administration of *trans*-polydatin; in situ perfusion of the rat small intestine and liver with *trans*-polydatin yielded the same result. The $AUC_{0-\infty}$ of *trans*-polydatin and its metabolites increased in a dose dependent manner following oral administration of *trans*-polydatin. This indicates that in the rats, *trans*-polydatin is absorbed in a dose-dependent manner and undergoes extensive first-pass deglycosylation and glucuronidation. Orally administered *trans*-polydatin, therefore, is metabolized primarily to resveratrol in the small intestine and liver, where it is further metabolized to the glucuronidated resveratrol.

KEYWORDS: Glucuronides; liquid chromatography−mass−mass; first-pass metabolism; pharmacokinetic; resveratrol; *trans*-polydatin

INTRODUCTION

Several epidemiological studies have shown that a moderate consumption of red wine is related to a reduced incidence of heart disease and cancer (*1*, *2*). Polyphenols have been found in a number of plant species, but grapes and wine are the most important foods containing these substances. In red wine, one of the most significant compounds in terms of possible health benefits is *trans*-resveratrol (*trans*-3,5,4′-trihydroxystilbene). Indeed, resveratrol has been reported to have anticarcinogenic, antioxidant, and cardioprotective activities (*3*). It may exert a protective effect against atherogenesis through its antioxidant properties. Although there is considerable evidence that *trans*-resveratrol possesses strong biological activity, wine has a low level of *trans*-resveratrol in comparison to its glucoside *trans*-polydatin (piceid, *trans*-3,5,4′-trihydroxylstilbene-3-mono-D-glycoside). In fact, the level of *trans*-polydatin in red wine is 10 times greater than the level of *trans*-resveratrol (*4*). Therefore, *trans*-polydatin is the main dietary source of *trans*-resveratrol in red wine. Additionally, previous studies have shown that *trans*-polydatin can inhibit platelet aggregation, improve microcirculation, alleviate tissue-organ damage induced by ischemia reperfusion, lower blood cholesterol, and suppress lipid peroxide formation (*5*, *6*).

The absorption and metabolism of resveratrol have been extensively investigated by different research approaches. The oral bioavailability of resveratrol is almost zero due to rapid and extensive metabolism and the subsequent formation of various metabolites such as resveratrol-glucuronides and resveratrol-sulfates (*7*). It was reported that resveratrol-glucuronides were the main metabolites after resveratrol was orally administered to Wistar rats (*8*). In vitro studies indicated that *trans*-polydatin was deglycosylated in Caco-2 cells; the resulting aglycone was metabolized into *trans*-resveratrol-3-*O*-*β*-glucuronide and to a lesser extent into *trans*-resveratrol-4′-*O*-*β*-glucuronide. When *trans*-polydatin was incubated with Caco-2 cells, *trans*-resveratrol was detected on both apical and basolateral sides (*9*). In vivo studies have shown that *trans*-polydatin, *trans*-resveratrol-3-*O*-*β*-glucuronide, and *trans*-resveratrol are detectable in plasma after oral administration of *trans*-polydatin (150 mg kg^{-1}) to Wistar rats (*10*). Moreover, when *trans*-polydatin (85.5 mg/70 kg of body weight) was orally administered to healthy volunteers, *trans*-resveratrol-3-sulfate, *trans*-resveratrol-3,4′-disulfate, *trans*-resveratrol-3,5-disulfate, *trans*-resveratrol-3-glucuronide, and *trans*-resveratrol-4′-glucuronide were identified in plasma and urine (*11*).

Although the metabolism of *trans*-polydatin has been investigated, there exist no quantitative data reporting the dose-dependent

*Author to whom correspondence should be addressed (e-mail: qbmei@fmmu.edu.cn).

 Published on Web 04/27/2009

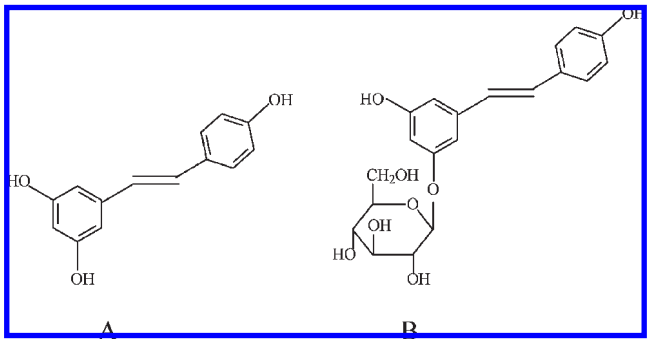

Figure 1. Chemical structures of *trans*-resveratrol (**A**) and *trans*-polydatin (**B**).

absorption and first-pass metabolism of *trans*-polydatin in vivo. In this paper, the dose-dependent absorption and metabolism of *trans*-polydatin were studied in rats, using in situ perfusion of rat small intestine and liver to investigate the products of first-pass metabolism.

MATERIALS AND METHODS

Materials. High-purity (>99%) *trans*-polydatin and resveratrol (**Figure 1**) were kindly donated by Xi'an Haotian Bioengineering Technology Co., Ltd., China. Genistein and glucuronidase (catalog no. G-0251) were purchased from Sigma Chemical Co. Acetonitrile and methanol were of HPLC grade, and other chemicals used were of analytical reagent grade. Sprague−Dawley rats (200 ± 20 g) were purchased from the Experimental Animal Research Center, the Fourth Military Medical University (Xi'an, China). The animals were allowed water and laboratory chow ad libitum. A 12 h light/dark cycle was used. Rats were fasted for 12 h prior to experimental use. All animal procedures were performed in accordance with protocols approved by the University Animal Care and Use Committee.

Administration of *trans*-Polydatin. In this study, the oral dose of *trans*-polydatin was determined according to published reports on the efficacy and metabolism of polydatin or resveratrol (*5*, *10*, *12*). *trans*-Polydatin was suspended in 0.5% carboxymethylcellulose sodium solution, administered to rats by gavage at doses of 50, 100, and 300 mg kg^{-1}. There were 72 rats in each dosage group. The rats were anesthetized by diethyl ether, and 2 mL blood samples were drawn from the abdominal aorta 0.17, 0.33, 0.5, 1, 2, 4, 6, 8, 12, 16, 24, and 36 h after each dosing. Blood samples were heparinized and plasma was separated by centrifugation (7 min, 4 °C, 2000*g*). Six new rats were sampled for each sampling time.

In Situ Perfusion of Rat Small Intestine. To investigate the metabolism of *trans*-polydatin in the small intestine, the in situ perfused rat small intestine model was used as previously described (*13*). The *trans*-polydatin concentration in perfusate was in accordance with the previously published papers (*14*, *15*). Briefly, the Sprague−Dawley rats were anesthetized by using an intraperitoneal injection of xylazine/ketamine (15/75 mg kg^{-1}). The rat small intestine was exposed by midline incision, and a 7−11 cm long segment of the intestine from 5 cm below the ligament of Treitz was identified and separated. Silicone tubing (i.d. = 3.0 mm, o.d. = 5.0 mm) was placed inside both ends of the segment, and the tube at the proximal side was connected to a peristaltic pump for luminal perfusion. The segment was then perfused (0.5 mL min^{-1}) with warm normal saline containing 50 μM *trans*-polydatin. A polyethylene cannula (i.d. = 0.5 mm, o.d. = 0.8 mm), connected to a peristaltic pump for the vascular perfusion, was inserted into the superior mesenteric artery. The single-pass perfusion of perfusate, consisting of Krebs−Ringer bicarbonate buffer (pH 7.4) including 5.5 mM D-glucose, 3% BSA, 2.5% dextran-70, and 0.8 mM L-glutamine, gases with 95% O_2 and 5% CO_2, was begun immediately at 2.0 mL min^{-1}. The mesenteric vein for collecting buffer from the specified segment of intestine was cannulated with 6 cm long polyethylene tubing (i.d. = 0.86 mm, o.d. = 1.27 mm). To maintain a constant temperature of the perfusate, the inlet cannula was insulated and kept warm by a 37 °C water bath. Samples obtained from the outlet of the mesenteric vein and luminal aliquots were collected into the tubes every 10 min.

Table 1. HPLC Gradient Condition

time (min)	acetonitrile (A, %)	water (B, %)	flow rate (mL/min)	curve
0	30	70	0.2	1
2	60	40	0.2	6
6	100	0	0.2	6
14	30	70	0.2	1

Table 2. Mass Spectrum Condition

compound	precursor	daughter	dwell time (s)	capillary voltage (kV)	cone voltage (V)	collision energy (eV)
polydatin	389	227	0.4	3.5	25	13
resveratrol	227	143	0.4	3.5	45	23
genistein	269	133	0.4	3.5	32	5

In Situ Perfusion of Rat Liver. To investigate the metabolism of *trans*-polydatin in liver, the in situ perfused rat liver preparation was used as described previously (*16*). The *trans*-polydatin concentration in perfusate was determined according to the *trans*-polydatin concentration in the plasma after oral administration of *trans*-polydatin (50 mg kg^{-1}) and the previous literature (*17*). Briefly, Sprague−Dawley rats were anesthetized using an intraperitoneal injection of xylazine/ketamine (15/75 mg kg^{-1}). The portal vein and superior vena cava were cannulated using an intravenous 16 or 18 gauge catheter, respectively. The laparatomized rats were heparinized with 500 units of heparin injected into the inferior vena cava. The perfusions were conducted using freshly prepared Krebs−Henseleit buffer (118 mM NaCl, 4.5 mM KCl, 2.75 mM $CaCl_2$, 1.19 mM KH_2PO_4, 1.18 mM $MgSO_4$, and 25 mM $NaHCO_3$, equilibrated with 95% O_2/5% CO_2, pH 7.4) with a constant flow rate of 10 mL min^{-1} using a peristaltic pump through the portal vein. The effluent perfusate was collected from the superior vena cava. To maintain a constant temperature of the perfusate, the inlet cannula was insulated and kept warm by a 37 °C water bath. The final concentration of *trans*-polydatin in perfusate was 1.5 μM.

Sample Pretreatment. To detect the free *trans*-polydatin and resveratrol, 0.25 mL of plasma (or perfusate) and 100 μL of genistein solution (internal standard, 0.4 mg L^{-1}) were added into the tubes. The samples were extracted twice with 2.0 mL of ethyl acetate. The organic phase of each sample was transferred to a clean tube and evaporated to dryness at 30 °C under a gentle stream of nitrogen in the ventilation cabinet. The residue of each sample was dissolved in 50 μL of methanol, and 10 μL was taken for LC-MS/MS analysis. Glucuronides were identified and quantified on the basis of enzymatic hydrolysis with glucuronidase. Briefly, 0.2 mL of glucuronidase solution (2000 units mL^{-1} in 0.17 mol L^{-1} ammonium acetate, pH 4.6) was added to 0.25 mL of plasma and incubated at 37 °C for 2 h in a shaking water bath. Preliminary studies showed that this protocol ensured the complete hydrolysis of the glucuronides (*13*). Next, the samples were extracted and the total *trans*-polydatin and resveratrol in each sample were detected as described above. Free *trans*-polydatin and resveratrol were deducted from the total amount of *trans*-polydatin and resveratrol to calculate the amount of glucuronidated *trans*-polydatin and glucuronidated resveratrol in each plasma sample.

Analytical Method. *trans*-Polydatin and its metabolites were analyzed as previously described (*18*). A Quattro Premier liquid chromatograph−mass/mass (LC-MS/MS) system (Waters Corp., Milford, MA) operating under Masslynx 4.1 software was used. Briefly, an XTerra C_{18} analytical column (150 × 2.1 mm, 5 μm, Waters Corp.) was used with the mobile phase gradient elution of acetonitrile/water. Eluant A was acetonitrile, and eluant B was water. The gradient was run from 30% A to 100% B over 6 min as shown in **Table 1**. An electrospray ionization−mass spectrometry (ESI^-) source was used as detector and was operated in negative ion mode in selected multiple reaction monitoring (MRM) mode with the transitions of *m*/*z* 389−227 (*trans*-polydatin) and *m*/*z* 227−143 (resveratrol) used as quantifier ion, respectively, as shown in **Table 2**.

Statistical Method. The area under the curve (AUC_{0-t}) was calculated using the linear trapezoidal rule from zero to the last plasma drug

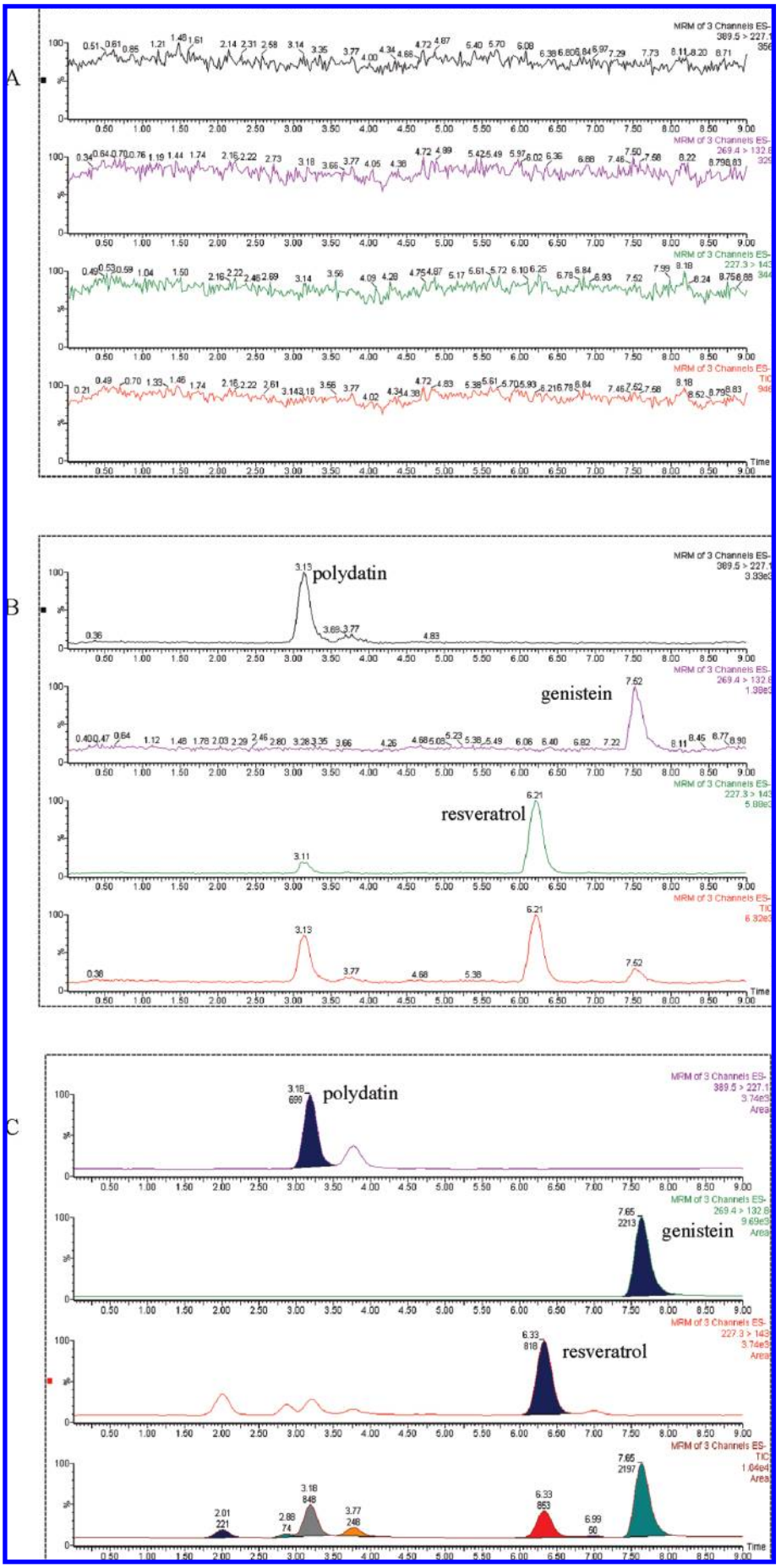

Figure 2. Typical LC-MS/MS chromatograms of a plasma blank (**A**), a plasma blank spiked with *trans*-polydatin, resveratrol, and internal standard (**B**), a plasma sample obtained from a rat following oral administration 300 mg kg^{-1} of *trans*-polydatin (**C**), and the same plasma sample treated with glucuronidase (**D**).

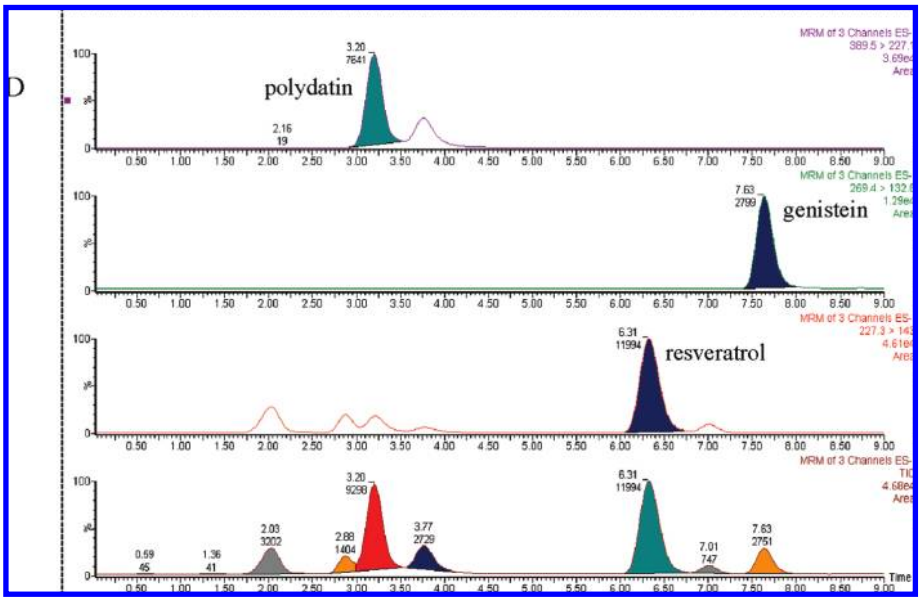

Figure 2. (Continued).

concentration. By semilogarithm graphic rules, terminal elimination rate constants (K_e) were estimated with least-squares regression of values in the terminal log-linear region of plasma concentration−time curves; $t_{1/2}$ was calculated as $0.693/K_e$. $AUC_{0-\infty}$ was calculated as $AUC_{0-t} + C_t/K_e$, where C_t is the last detectable plasma concentration and t is the time at which this concentration occurred. Peak concentration (C_{max}) and T_{max} were obtained from observed data. Statistical significance was determined with one-way analysis of variance (ANOVA); $P < 0.05$ was regarded as significant difference.

RESULTS

Validation of Analytical Method. Under the optimized chromatographic condition, *trans*-polydatin, resveratrol, and internal standard (IS) were clearly separated chromatographically with retention times of 3.1, 6.2, and 7.5 min, respectively. No significant interference between the analytes or the internal standard with endogenous substances was detected (**Figure 2A**,**B**). The peak area of *trans*-polydatin and resveratrol increased in the glucuronidase-treated samples (**Figure 2D**) when compared to the results of chromatograms of untreated samples (**Figure 2C**). Meanwhile, the peak area of the IS in the two samples exhibited almost no change. Through this method, we identified and quantified the glucuronoconjugate of *trans*-polydatin and resveratrol in blood and perfusate sample. The precision of the analytical method, expressed as the intraday and interday relative standard deviations (RSDs), was below 7.1% for quality control samples. The accuracy, expressed as the relative error (RE), was within ±5.7% for all analytes. The recovery of *trans*-polydatin and resveratrol with this analytical method varied from 92 to 110%. The lower limit of quantification (LLOQ) is 0.4 ng mL^{-1}.

Absorption of *trans*-Polydatin at Different Doses in Rats. When orally administered to rats, *trans*-polydatin was absorbed rapidly. The concentration−time curve of *trans*-polydatin is shown in **Figure 3A**. The results of the noncompartmental pharmacokinetic analysis are summarized in **Table 3**. The percentage of free *trans*-polydatin in the total drug (free *trans*-polydatin + metabolites) detected in the plasma at different doses is shown in the Supporting Information (Table S1). As the oral dose increased from 50 to 300 mg kg^{-1}, the peak concentration (C_{max}) and $AUC_{0-\infty}$ increased in a dose-dependent manner (R^2 = 0.9963 and 0.9997, respectively); also, the $t_{1/2}$ was prolonged.

Pharmacokinetics of *trans*-Polydatin Metabolites in Rats at Different Doses. After oral administration of *trans*-polydatin, high levels of resveratrol, glucuronidated *trans*-polydatin, and glucuronidated resveratrol were detected in the plasma. The concentration−time curve of the metabolites is shown in **Figure 3**. The resveratrol concentration in the plasma reached its first peak (C_{max1}) at 20 min and its second peak (C_{max2}) at 400 min. In parallel with the concentration of resveratrol, glucuronidated resveratrol concentration in plasma reached its first peak (C_{max1}) at 30 min and its second peak (C_{max2}) at 400 min. As the oral dose increased from 50 to 300 mg kg^{-1}, the peak concentration (C_{max1}) and $AUC_{0-\infty}$ of resveratrol, glucuronidated *trans*-polydatin, and glucuronidated resveratrol increased in a dose-dependent manner (R^2 = 0.797 and 0.994 for resveratrol; R^2 = 0.999 and 0.992 for glucuronidated *trans*-polydatin; R^2 = 0.998 and 0.993 for glucuronidated resveratrol), and the $t_{1/2}$ was prolonged. The results of the noncompartmental pharmacokinetic analysis are summarized in **Tables 3** and **4**. The percentage of free resveratrol, glucuronidated *trans*-polydatin, and glucuronidated resveratrol in the total drug (free *trans*-polydatin + metabolites) determined in plasma at different doses is shown in the Supporting Information (Tables S2−S4).

First-Pass Metabolism of *trans*-Polydatin in Rat Small Intestine and Liver. In control perfusion experiments with *trans*-polydatin free perfusate, *trans*-polydatin and its metabolites were not detected in vascular compartments. *trans*-Polydatin, resveratrol, glucuronidated resveratrol, and glucuronidated *trans*-polydatin were detected in vascular compartments within 10 min after perfusion of *trans*-polydatin in situ rat small intestine. The amount of *trans*-polydatin and its metabolites in the vascular effluent perfusate increased in a time-dependent manner (**Figure 4**). The percentage of metabolites in the total drug (*trans*-polydatin + metabolites) detected in vascular compartments at different time points is shown in the Supporting Information (Table S5). A significantly higher percentage of glucuronidated *trans*-polydatin occurred within 60 min after perfusion in comparison with either glucuronidated resveratrol or resveratrol ($P < 0.05$ vs glucuronidated resveratrol; $P < 0.01$ vs resveratrol).

The pattern of metabolism of *trans*-polydatin in rat liver was similar to that seen in rat small intestine. The amounts of resveratrol, glucuronidated resveratrol, and glucuronidated *trans*-polydatin in the effluent perfusate from the superior vena cava increased in a time-dependent manner (**Figure 5**). The levels of *trans*-polydatin and its metabolites at each time point

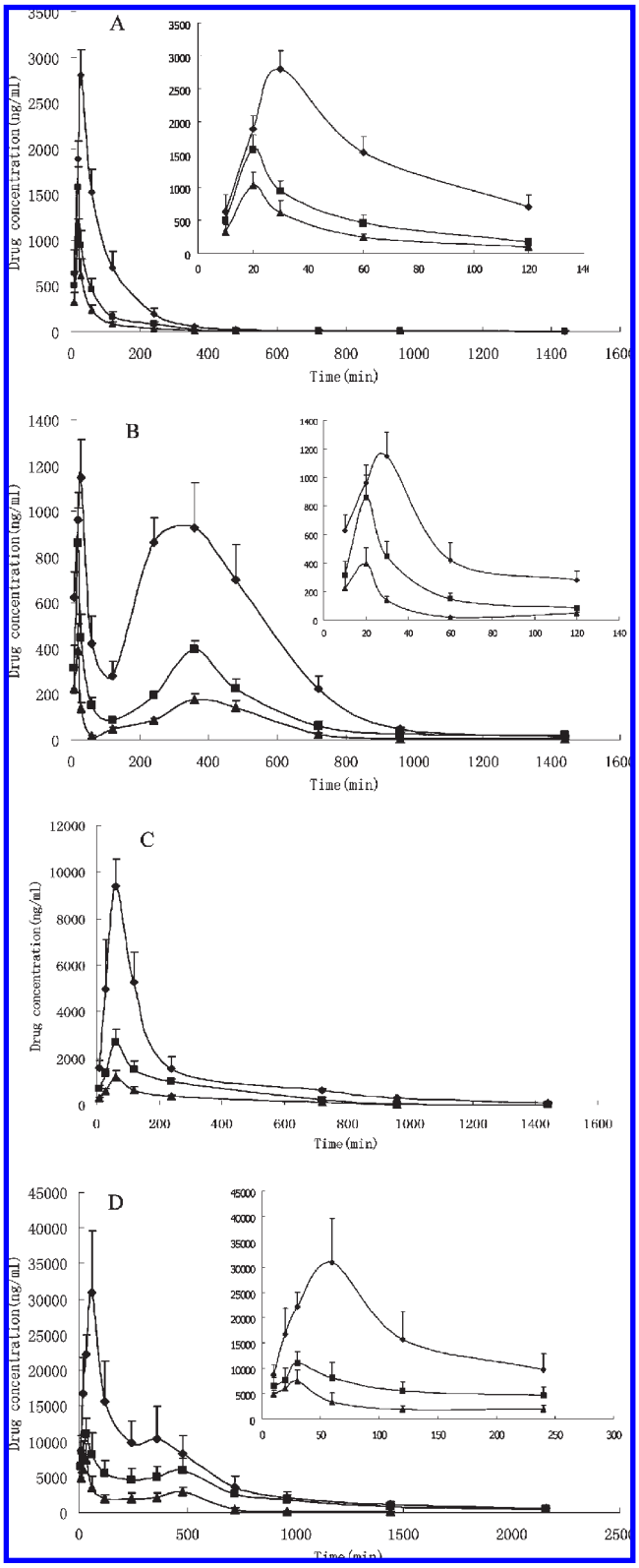

Figure 3. Concentration−time curves for *trans*-polydatin (**A**), resveratrol (**B**), glucuronidated *trans*-polydatin (**C**), and glucuronidated resveratrol (**D**) after oral administration of different doses of *trans*-polydatin: (◆) 300 mg kg^{-1}; (■) 100 mg kg^{-1}; (▲) 50 mg kg^{-1}. Data are mean ± SD, $n = 6$.

expressed as a percentage of the total concentration of *trans*-polydatin and its metabolite in the effluent perfusate are shown in the Supporting Information (Table S6). Glucuronidated resveratrol is the main metabolite detected in the effluent perfusate from the superior vena cava when compared to either glucuronidated *trans*-polydatin or resveratrol ($P < 0.02$ vs glucuronidated *trans*-polydatin; $P < 0.01$ vs resveratrol), which is different from the metabolism of *trans*-polydatin in rat small intestine. At any time point during perfusion, only small amounts of resveratrol were detected in the effluent perfusate.

DISCUSSION

Our study indicates that *trans*-polydatin can be absorbed and efficiently deglycosylated and glucuronidated in rats. *trans*-Polydatin, resveratrol, glucuronidated resveratrol, and glucuronidated *trans*-polydatin were detected in plasma after oral administration of *trans*-polydatin. To our knowledge, there are no previous reports of the formation of glucuronidated *trans*-polydatin when *trans*-polydatin is metabolized in Caco-2 cells, Wistar rats, and humans. It is reported that the efflux pump MRP2 (multidrug resistance associated protein 2) is involved in the apical efflux of both *trans*-polydatin and *trans*-resveratrol by Caco-2 cells (*9*, *19*). In this study, when C_{max} was normalized with dose, the value of *trans*-polydatin, resveratrol, and glucuronidated resveratrol decreased when the dose increased; meanwhile, the value of glucuronidated *trans*-polydatin increased with the dose. This implies that the absorption (or bioavailability) of *trans*-polydatin decreased at high dose, and the metabolism of *trans*-polydatin is nonlinearly dose-dependent in rats. When the dose of *trans*-polydatin increased from 50 to 300 mg kg^{-1}, the $t_{1/2}$ and t_{max} of *trans*-polydatin were prolonged. Another study has shown that after polydatin was intravenously administered to rats at doses of 10, 20, and 30 mg kg^{-1}, $t_{1/2}$ was 71.4, 90.4, and 95.0 min and $AUC_{0-\infty}$ was 807.54, 953.73, and 1919.30 mg min L^{-1} (*20*). These data indicate that elimination of orally administered *trans*-polydatin is likely limited by absorption rate. Moreover, the absorption and excretion of resveratrol in mice after oral ingestion of grape juice preparations was also investigated. The cumulative amounts of resveratrol excreted in the urine of the mice receiving concentrated grape juice for 4 days were 2.3% of the ingested doses. Plasma levels of resveratrol, however, were not detected (*21*). Interestingly, after *trans*-polydatin (85.5 mg/70 kg of body weight) was orally administered to healthy volunteers at a single dose, *trans*-resveratrol-sulfates are the dominant conjugates in plasma and urine. Neither *trans*-polydatin nor resveratrol was detected in the urine or the plasma samples (*11*). Taken together, this implies that the absorption and metabolism of *trans*-polydatin may be different between mice, rats, and humans.

When *trans*-polydatin was orally administered to the rats (300 mg kg^{-1}), the ratio of exposures (AUC_{0-t}) of *trans*-polydatin to the total drug (*trans*-polydatin + metabolites) detected in the plasma is 1.6%; the ratio of glucuronidated *trans*-polydatin to the total drug determined in plasma is 10.7%; the ratio of resveratrol to total drug detected in plasma is 3.7%; the ratio of glucuronidated resveratrol to total drug detected in plasma is 84%. These results indicate that the proportion of *trans*-polydatin in plasma was very small and that considerable amounts of resveratrol are formed after oral administration of *trans*-polydatin. Previous work demonstrated that when *trans*-polydatin was orally administered to rats at a dose of 240 mg kg^{-1}, considerable amounts of resveratrol were detected in the contents of the intestine and cecum (*22*). The results of in situ perfusion of the rat small intestine and liver also indicate that the hydrolysis of *trans*-polydatin by β-glucosidases and the glucuronidation of *trans*-polydatin and resveratrol by UDP-glucuronosyltransferases can occur in the intestine and the liver, thus allowing the quantity of *trans*-resveratrol available from the diet to be greater. The in vivo bioactivity of *trans*-polydatin may partially result from its metabolite (resveratrol). Previous study shows that there are two

Table 3. Main Pharmacokinetic Parameters of *trans*-Polydatin and Resveratrol in Rat after Oral Administration of Different Doses of *trans*-Polydatin[a]

	trans-polydatin			resveratrol		
parameter	50 mg kg^{-1}	100 mg kg^{-1}	300 mg kg^{-1}	50 mg kg^{-1}	100 mg kg^{-1}	300 mg kg^{-1}
$t_{1/2}$ (min)	120.2	185.0	285.3	107	301	425
T_{max} (min)	20	20	30	20	20	30
C_{max1} (ng mL^{-1})	1033	1280	2800	393	858	1147
C_{max2}	NA	NA	NA	177	395	929
AUC_{0-t} (mg min L^{-1})	54	86	228	77	123	490
$AUC_{0-\infty}$(mg min L^{-1})	55	87	230	78	132	524
C_{max1}/dose	21	13*	9**,#	8	9	4**
C_{max2}/dose	NA	NA	NA	4	4	3
$AUC_{0-\infty}$/dose	1.1	0.9	0.8	1.6	1.3	1.7

[a] $t_{1/2}$, elimination half-life; T_{max}, time to reach maximum plasma concentration; C_{max}, maximum plasma concentration; AUC, area under curve. NA, not applicable. *, $P < 0.05$, and **, $P < 0.02$, vs 50 mg kg^{-1}; #, $P < 0.05$, vs 12.5 mg kg^{-1}.

Table 4. Main Pharmacokinetic Parameters of Glucuronidated *trans*-Polydatin and Glucuronidated Resveratrol in Rat after Oral Administration of Different Doses of *trans*-Polydatin[a]

	glucuronidated *trans*-polydatin			glucuronidated resveratrol		
parameter	50 mg kg^{-1}	100 mg kg^{-1}	300 mg kg^{-1}	50 mg kg^{-1}	100 mg kg^{-1}	300 mg kg^{-1}
$t_{1/2}$ (min)	385	433	578	213	496	545
t_{max} (min)	60	60	60	30	30	60
C_{max1} (ng mL^{-1})	1165	2687	9392	7426	11094	30900
C_{max2}	NA	NA	NA	2835	4918	10404
AUC_{0-t} (mg min L^{-1})	283	705	1712	1888	4560	11883
$AUC_{0-\infty}$(mg min L^{-1})	291	714	1779	1919	4817	12298
C_{max1}/dose	23	27	31*	148	111*	101**
C_{max2}/dose	NA	NA	NA	57	49	40
$AUC_{0-\infty}$/dose	5.8	7.1	5.9	38.4	48.2	41.0

[a] $t_{1/2}$, elimination half-life; t_{max}, time to reach maximum plasma concentration; C_{max}, maximum plasma concentration; AUC, area under curve. NA, not applicable. *, $P < 0.05$, and **, $P < 0.02$, vs 50 mg kg^{-1}.

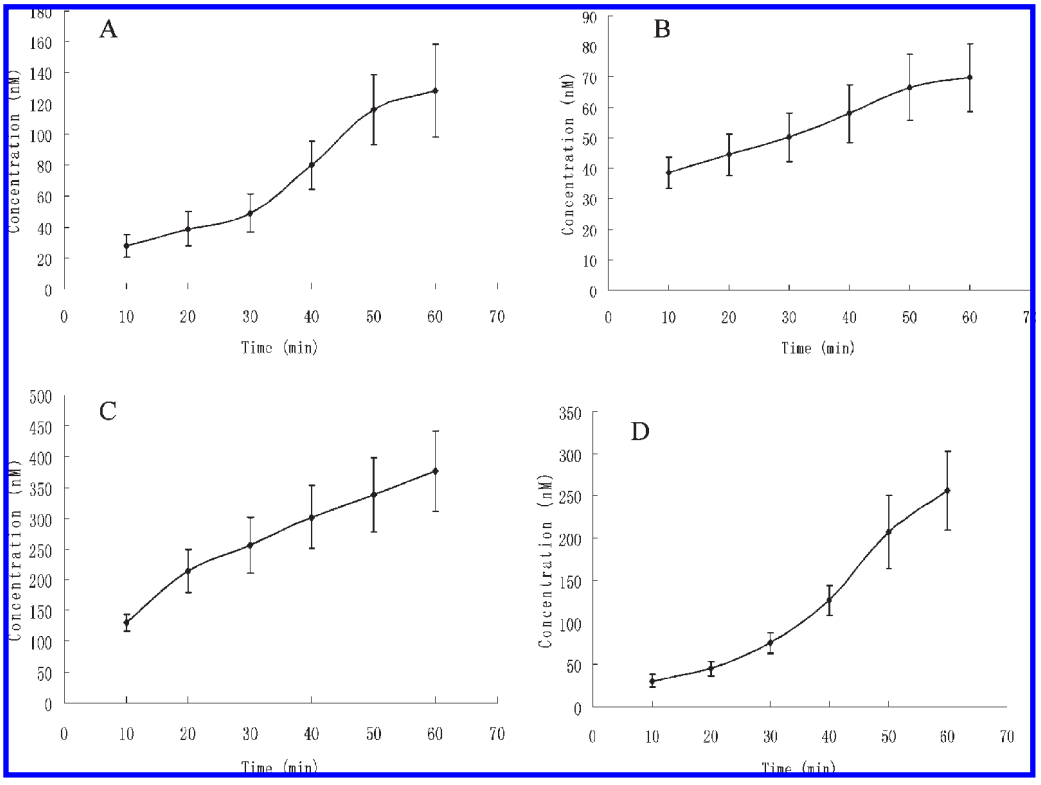

Figure 4. *trans*-Polydatin and its metabolites in the vascular compartments after in situ perfusion of rat small intestine with *trans*-polydatin (50 μM): (**A**)*trans*-polydatin; (**B**) resveratrol; (**C**) glucuronidated *trans*-polydatin; (**D**) glucuronidated resveratrol. Data are mean ± SD, $n = 6$.

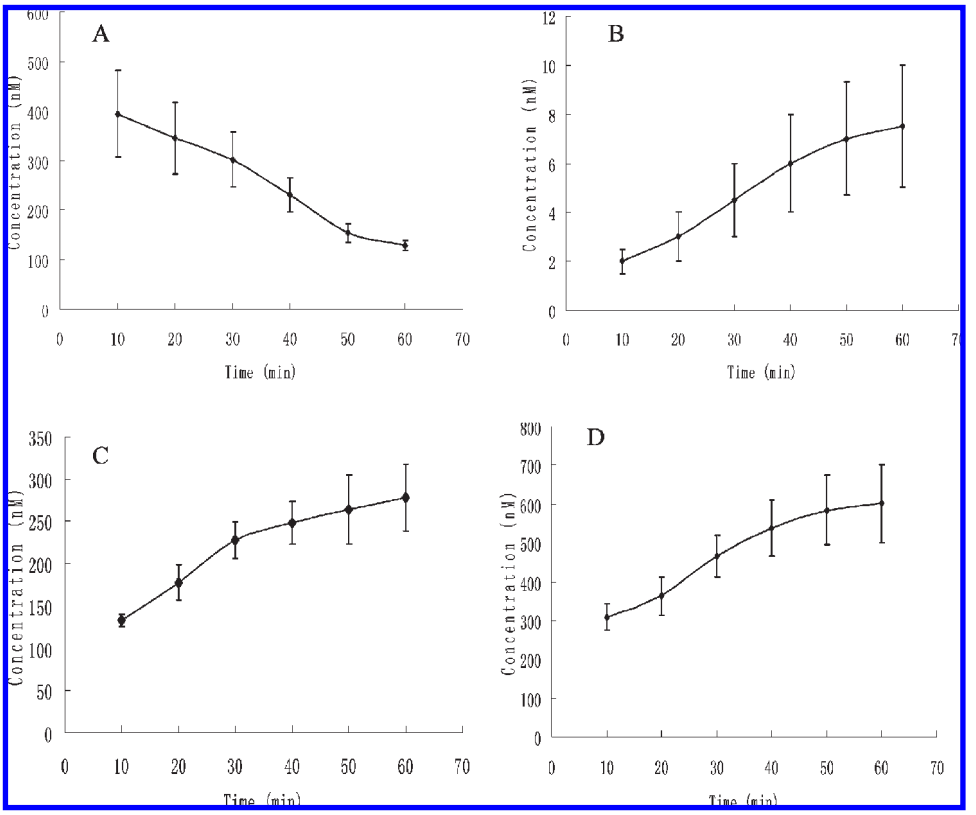

Figure 5. *trans*-Polydatin and its metabolites in effluent perfusate from the superior vena cava after in situ perfusion rat liver with *trans*-polydatin (1.5 μM): (**A**) *trans*-polydatin; (**B**) resveratrol; (**C**) glucuronidated *trans*-polydatin; (**D**) glucuronidated resveratrol. Data are mean ± SD, $n = 6$.

possible pathways by which *trans*-polydatin is hydrolyzed in the intestine. The first is a cleavage by the cytosolic-β-glucosidase (CBG), after passing the brush-border membrane by SGLT1 (sodium dependent glucose transport 1). The second is deglycosylation on the luminal side of the epithelium by the membrane-bound enzyme lactase phlorizin hydrolase (LPH), followed by passive diffusion of the released aglycone, which is further metabolized inside the cells into two glucuronides (*23*). Recent studies have shown that the transport of resveratrol-glucuronide conjugate and resveratrol-sulfate conjugate is mediated by multidrug resistance protein 3 (MRP3, ABCC3) and/or breast cancer resistance protein (BCRP, ABCG2), which are located in the basolateral and apical membranes of enterocytes, respectively. The absence of *Mrp3* in mice results in altered disposition of resveratrol-3-glucuronide and its parent compound resveratrol, leading to a reduced percentage of resveratrol being excreted via the urine in *Mrp3(−/−)* mice (*24*).

Compared with glucuronidated *trans*-polydatin, glucuronidated resveratrol is the main glucuronoconjugate after oral administration of *trans*-polydatin to rats. It has been documented that resveratrol, like other polyphenols, is extensively metabolized via the glucuronidation pathway (*15*, *25*, *26*). The reaction is catalyzed by the UDP-glucuronosyltransferases (UGT), a multigenic family of enzymes that transfer a glucuronic acid moiety from the donor substrate, UDP-glucuronic acid (UDP-GlcUA), to phenolic groups of the substrate, leading to the formation of *O*-glucuronides, which are readily excreted in urine. It was reported that human liver microsomal UGTs could actively glucuronidate both the *trans*- and *cis*-isomers of resveratrol (*27*). The reaction was regioselective, leading to the formation of 3-*O*- and 4′-*O*-glucuronides, with no 5-*O*-glucuronide being formed. *trans*-Resveratrol-3-*O*-β-glucuronide is the main glucuronoconjugate in human liver microsomes. Glucuronidation of resveratrol was also stereoselective, as the *cis*-isomer was glucuronidated at a faster rate compared with the *trans*-isomer. However, β-glucuronidases, which are widely expressed in human organs, tissues, and body fluids, might modulate the rate of glucuronides and release active parent aglycone (*28*). This pathway would increase the amount of resveratrol and therefore enhance its effectiveness in humans.

The results of in situ perfusion of rat liver with polydatin indicated that only small amounts of resveratrol were detected in the effluent perfusate. The hepatic metabolism and the transport system for resveratrol were examined in isolated perfused livers from Wistar and *Mrp2*-deficient TR(−) rats. The results show that resveratrol was dose-dependently metabolized to several resveratrol-glucuronide conjugates and resveratrol-sulfate conjugates. Also, a small amount of resveratrol was detected in the effluent perfusate. MRP2 extensively mediates the biliary excretion of resveratrol-glucuronides but only partly that of resveratrol-sulfates (*17*).

There are two distinct peaks in the plasma concentration−time curve of resveratrol and glucuronidated resveratrol, which indicate enterohepatic recirculation, as has already been suggested by several studies (*29*, *30*). Furthermore, according to the time at which peaks 1 and 2 occurred, the presence of distinct peaks 1 and 2 may also show a region dependent absorption rate in the rat gastrointestinal tract. Whether or not enterohepatic recirculation of resveratrol and glucuronidated resveratrol significantly contributes to the overall pharmacological activity of resveratrol remains to be determined.

To our knowledge, this is the first study assessing the dose-dependent absorption and first-pass metabolism of *trans*-polydatin in vivo. The results indicate *trans*-polydatin can be absorbed in a dose-dependent manner and undergoes extensive first-pass deglycosylation and glucuronidation in rats. The main glucuronide conjugate in rat is resveratrol-glucuronide after oral administration of *trans*-polydatin. High levels of resveratrol are formed

after oral administration of *trans*-polydatin, increasing the quantity of *trans*-resveratrol available from the diet.

Although many studies have implicated a role of resveratrol in disease prevention, its role in human health as a dietary nonnutritional bioactive compound is controversial. This is because of its low abundance in the diet and its low bioavailability. To understand the beneficial effects of consuming resveratrol or polydatin on humans, some essential questions remain to be answered: (1) What are the optimal dosages of resveratrol or polydatin that should be consumed to induce a health benefit? (2) Is long-term supplementation with high doses of resveratrol or polydatin safe?

Supporting Information Available: Tables S1−S6, percentages of *trans*-polydatin, resveratrol, glucuronidated *trans*-polydatin, glucuronidated reseveratol, and *trans*-polydatin metabolites in plasma, vascular compartments, and effluent perfusate. This material is available free of charge via the Internet at http://pubs.acs.org.

LITERATURE CITED

(1) Gronbaek, M.; Becker, U.; Johansen, D.; Gottschau, A.; Schnohr, P.; Hein, H. O.; Jensen, G.; Sorensen, T. I. Type of alcohol consumed and mortality from all causes, coronary heart disease, and cancer. *Ann. Intern. Med*. **2000**, *133*, 411–419.

(2) Renaud, S.; de Lorgeril, M. Wine, alcohol, platelets, and the French paradox for coronary heart disease. *Lancet* **1992**, *339*, 1523–1526.

(3) Jang, M.; Cai, L.; Udeani, G. O.; Slowing, K. V.; Thomas, C. F.; Beecher, C. W.; Fong, H. H.; Farnsworth, N. R.; Kinghorn, A. D.; Mehta, R. G.; Moon, R. C.; Pezzuto, J. M. Cancer chemopreventive activity of resveratrol, a natural product derived from grapes. *Science* **1997**, *275*, 218–220.

(4) Ribeiro de Lima, M. T.; Waffo-Téguo, P.; Teissedre, P. L.; Pujolas, A.; Vercauteren, J.; Cabanis, J. C.; Mérillon, J. M. Determination of stilbenes *trans*-astringin, *cis*- and *trans*-piceid, and *cis*- and *trans*-resveratrol in Portuguese wines. *J. Agric.Food. Chem*. **1999**, *47*, 2666–2670.

(5) Cheng, Y.; Zhang, H. T.; Sun, L.; Guo, S.; Ouyang, S.; Zhang, Y.; Xu, J. Involvement of cell adhesion molecules in polydatin protection of brain tissues from ischemia-reperfusion injury. *Brain Res*. **2006**, *1110*, 193–200.

(6) Du, J.; Sun, L. N.; Xing, W. W.; Huang, B. K.; Jia, M.; Wu, J. Z.; Zhang, H.; Qin L. P. Lipid-lowering effects of polydatin from Polygonum cuspidatum in hyperlipidemic hamsters. *Phytomedicine* 2008 [Dec 21, Epub ahead of print].

(7) Wenzel, E.; Somoza, V. Metabolism and bioavailability of *trans*-resveratrol. *Mol. Nutr. Food Res*. **2005**, *49*, 472–481.

(8) Wenzel, E.; Soldo, T.; Erbersdobler, H.; Somoza, V. Bioactivityand metabolism of *trans*-resveratrol orally administered to Wistar rats. *Mol. Nutr. Food Res*. **2005**, *49*, 482–494.

(9) Henry, C.; Vitrac, X.; Decendit, A.; Ennamany, R.; Krisa, S.; Merillon, J. M. Cellular uptake and efflux of transpiceid and its aglycone *trans*-resveratrol on the apical membrane of human intestinal Caco-2 cells. *J. Agric. Food Chem*. **2005**, *53*, 798–803.

(10) Zhou, M.; Chen, X. Y.; Zhong, D. F. Simultaneous determination of *trans*-resveratrol-3-*O*-glucoside and its two metabolites in rat plasma using liquid chromatography with ultraviolet detection. *J. Chromatogr., B: Anal. Technol. Biomed. Life Sci*. **2007**, *854*, 219–223.

(11) Burkon, A.; Somoza, V. Quantification of free and protein-bound *trans*-resveratrol metabolites and identification of *trans*-resveratrol-C/O-conjugated diglucuronides-two novel resveratrol metabolites in human plasma. *Mol. Nutr. Food Res*. **2008**, *52*, 549–557.

(12) Marier, J. F.; Vachon, P.; Gritsas, A.; Zhang, J.; Moreau, J. P.; Ducharme, M. P. Metabolism and disposition of resveratrol in rats: extent of absorption, glucuronidation, and enterohepatic recirculation evidenced by a linked-rat model. *J. Pharmacol. Exp. Ther*. **2002**, *302*, 369–373.

(13) Teng, Z. H.; Zhou, S. Y.; Yang, R. T.; Liu, X. Y.; Liu, R. W.; Yang, X.; Zhang, B. L.; Yang, J. Y.; Cao, D. Y.; Mei, Q. B. Quantitation assay for absorption and first-pass metabolism of emodin in isolated rat small intestine using liquid chromatography−tandem mass spectrometry. *Biol. Pharm. Bull*. **2007**, *30*, 1628–1633.

(14) Kuhnle, G.; Spencer, J. P.; Chowrimootoo, G.; Schroeter, H.; Debnam, E. S.; Srai, S. K.; Rice-Evans, C.; Hahn, U. Resveratrol is absorbed in the small intestine as resveratrol glucuronide. *Biochem. Biophys. Res. Commun*. **2000**, *272*, 212–217.

(15) Andlauer, W.; Kolb, J.; Siebert, K.; Fürst, P. Assessment of resveratrol bioavailability in the perfused small intestine of the rat. *Drugs Exp.Clin.Res*. **2000**, *26*, 47–55.

(16) Cheung, K.; Hickman, P. E.; Potter, J. M.; Walker, N. I.; Jericho, M.; Haslam, R.; Roberts, M. S. An optimized model for rat liver perfusion studies. *J. Surg. Res*. **1996**, *66*, 81–89.

(17) Maier-Salamon, A.; Hagenauer, B.; Reznicek, G.; Szekeres, T.; Thalhammer, T.; Jäger, W. Metabolism and disposition of resveratrol in the isolated perfused rat liver: role of Mrp2 in the biliary excretion of glucuronides. *J. Pharm. Sci*. **2008**, *97*, 1615–1628.

(18) Yang, R. T.; Zhou, S. Y.; Zhang, X.; Teng, Z. H.; Zhang, B. L.; Liu, X. Y.; Yang, X.; Zhang, L. J.; Mei, Q. B. Simultaneous determination of polydatin and its metabolite in plasma by LC/MS/MS. *Chin. J. Anal. Chem*. **2007**, *35*, 1309–1314.

(19) Sergent, T.; Garsou, S.; Schaut, A.; Saeger, S. D.; Pussemier, L.; Peteghem, C. V.; Larondelle, Y.; Schneider, Y. J. Differential modulation of ochratoxin A absorption across Caco-2 cells by dietary polyphenols, used at realistic intestinal concentrations. *Toxicol. Lett*. **2005**, *159*, 60–70.

(20) Gao, S. H.; Fan, G. R.; Hong, Z. Y.; Yin, X. P.; Yang, S. L.; Wu, Y. T. HPLC determination of polydatin in rat biological matrices: application to pharmacokinetic studies. *J. Pharm. Biomed. Anal*. **2006**, *41*, 240–245.

(21) Meng, X.; Maliakal, P.; Lu, H.; Lee, M. J.; Yang, C. S. Urinary and plasma levels of resveratrol and quercetin in humans, mice, and rats after ingestion of pure compounds and grape juice. *J. Agric. Food Chem*. **2004**, *52*, 935–942.

(22) Zhang, W. T.; Qing, Li.; Zhu, M.; Huang, Q. W.; Jia, Y.; Bi, K. S. Direct determination of polydatin and its metabolite in rat excrement samples by high-performance liquid chromatography. *Chem. Pharm. Bull*. **2008**, *56*, 1592–1595.

(23) Henry-Vitrac, C.; Desmoulière, A.; Girard, D.; Mérillon, J. M.; Krisa, S. Transport, deglycosylation, and metabolism of *trans*-polydatin by small intestinal epithelial cells. *Eur. J. Nutr*. **2006**, *45*, 376–382.

(24) Van de Wetering, K.; Burkon, A.; Feddema, W.; Bot, A.; de Jonge, H.; Somoza, V.; Borst, P. Intestinal BCRP/Bcrp1 and MRP3/Mrp3 are involved in the pharmacokinetics of resveratrol. *Mol. Pharmacol*. 2008 [Dec 29, Epub ahead of print].

(25) Kuhnle, G.; Spencer, J. P.; Chowrimootoo, G.; Schroeter, H.; Debnam, E. S.; Srai, S. K.; Rice-Evans, C.; Hahn, U. Resveratrol is absorbed in the small intestine as resveratrol glucuronide. *Biochem. Biophys. Res. Commun*. **2000**, *272*, 212–217.

(26) Sabolovic, N.; Humbert, A. C.; Radominska-Pandya, A.; Magdalou, J. Resveratrol is efficiently glucuronidated by UDP-glucuronosyltransferases in the human gastrointestinal tract and in Caco-2 cells. *Biopharm. Drug Dispos*. **2006**, *27*, 181–189.

(27) Aumont, V.; Krisa, S.; Battaglia, E.; Netter, P.; Richard, T.; Mérillon, J. M.; Magdalou, J.; Sabolovic, N. Regioselective and stereospecific glucuronidation of *trans*- and *cis*-resveratrol in human. *Arch. Biochem. Biophys*. **2001**, *393*, 281–289.

(28) Sperker, B.; Backman, J. T.; Kroemer, H. K. The role of β-glucuronidase in drug disposition and drug targeting in humans. *Clin. Pharmacokinet*. **1997**, *33*, 18–31.

(29) Chen, J.; Lin, H. M.; Hu, M. Metabolism of flavonoids via enteric recycling: role of intestinal disposition. *J. Pharmacol. Exp. Ther*. **2003**, *304*, 1228–1235.

(30) Chen, J.; Wang, S.; Jia, X.; Bajimaya, S.; Lin, H.; Tam, V. H.; Hu, M. Disposition of flavonoids via recycling: comparison of intestinal versus hepatic disposition. *Drug Metab. Dispos*. **2005**, *33*, 1777–1784.

Received for review December 19, 2008. Revised manuscript received March 7, 2009. Accepted April 15, 2009.